Axial Tensile Strain/Transverse Compressive Stress Characteristics in High Strength Nb_3Sn Superconducting Wires(High Field Superconductors)

Sci. Rep. RITU A42 (1996) pp. 381-388
No. 2, May 1996

Axial Tensile Strain / Transverse Compressive Stress Characteristics in High Strength Nb_3Sn Superconducting Wires*

K. Katagiri[a], K. Watanabe[b], T. Kuroda[c], K. Kasaba[a], K. Noto[a], T. Okada[d] and O. Kohno[e]

[a][1]*Faculty of Engineering, Iwate University, Morioka 020, Japan*
[b]*Institute for Materials Research, Tohoku University, Sendai 980-77, Japan*
[c]*National Reseach Institute for Metals, 1-2-1 Sengen, Tsukuba 305, Japan*
[d]*Institute of Scientific and Industrial Research, Osaka University, Ibaraki 567, Japan*
[e]*Materials Research Laboratory, Fujikura Ltd., Tokyo 135, Japan*

(Received February 9,1996)

In order to improve the strain/stress characteristics of the critical current I_c, the availability of Nb matrix as well as the external CuNb reinforcing stabilizer to bronze processed Nb_3Sn multifilamentary superconducting wires has been examined up to the magnetic field of 14T and at a temperature of 4.2K. Although the axial tensile strain sensitivity of I_c does not change, the strain for peak I_c as well as the reversible strain limit increase in the wire with CuNb reinforcing stabilizer. Furthermore, the transverse compressive stress sensitivity of I_c decreases and the reversible stress limit increases. Although critical current density is not high, the Nb matrix Nb_3Sn wire shows higher tolerance to stress / strain. Correlation between axial strain effect and transverse compressive stress effect is briefly discussed.
KEYWORDS: Nb_3Sn superconducting wire, Strain effect, transverse stress effect, critical current, reinforcement

1. Introduction

The superconducting wire for high field large magnet experiences a large electromagnetic force in high fields. Such a force causes an axial tensile stress in the wire, and also a transverse compressive stress, if the radial displacement of the winding is suppressed by some constraints. There have been many attempts to reinforce superconducting wires so as to improve mechanical properties.[1-5] In wires for compact size high field magnets, in which the wind and react technique is used, the choice of a reinforcing material is important because the reinforcing material and the superconducting composites are heat treated collectively. In order to avoid a decrease in overall critical current density, addition of reinforcing material is not preferable. In some cases, the matrix of the wire is reinforced.[5] Replacement of stabilizer Cu to Ta[6] or to Al_2O_3 particle dispersed Cu[7] or to CuNb microcomposite[8-12] is promising, although the stability of the wire is decreased to some extent.[6,11]

In this context, a new bronze processed Nb_3Sn wire has been fabricated in which bronze cores are embedded in the Nb matrix, reverse in construction to the conventional bronze processed Nb_3Sn, although the stabilizing performance of Nb as well as critical current density are not good enough.[13] The principal aim of this wire fabrication is to examine the effect of the mechanical property of the matrix material on both axial and transverse stress / strain dependence of critical current I_c. On the other hand, the present authors showed that the CuNb reinforcing stabilizer changes not only mechanical properties but also the tensile strain characteristics of critical current I_c, especially, in the 0.2% proof stress and the strain to peak I_c.[11,12]

From the view point of improving the tensile strain / tranverse compressive stress characteristics of I_c, the availability of the Nb matrix as well as the external CuNb reinforcing stabilizer to bronze processed Nb_3Sn multifilamentary superconducting wires is examined in the magnetic fields up to 14 T at a temperature of 4.2K. Correlation between the tensile strain dependence and the transverse compressive strain dependence of I_c in the wires is also discussed.

2. Experimental

A Nb matrix multifilamentary Nb_3Sn superconducting wires [Nb_mNb_3Sn] was fabricated using a bronze process. The number of bronze cores imbedded in the Nb matrix is 15. For comparison, a conventional bronze processed multifilamentary Nb_3Sn wire [Bz_mNb_3Sn] was also prepared. On the other hand, a pair of multifilamentary Ti added Nb_3Sn superconducting wires with a CuNb reinforcing stabilizer and with a conventional Cu stabilizer for reference, CuNb/$(Nb,Ti)_3Sn$ and Cu/$(Nb,Ti)_3Sn$ wires, were prepared through a bronze process. The specifi-

*IMR, Report No. 2049

cations together with heat treatment conditions and the cross sectional views of the 4 kinds of wires are shown in Table 1(a),(b) and Fig.1. Wires of pure Cu and CuNb which were drawn into a diameter of 0.8 mm from the material used in the pair of superconducting wires were heat treated in the same condition as that in the superconducting wires.

Measurements of the axial strain dependence of I_c as well as the transverse compressive stress dependence of I_c were conducted at 4.2K, using two apparatus inserted in the 15T superconducting magnet in the Materials Research Institute, Tohoku University. The details of the testing apparatus have been already reported elsewhere.[14,15] The I_c was determined by a 4 probe method using a nominal electrical field criterion of 1μV/cm based on the actual tap separation of 5 mm within 17.5 mm gauge length. In the transverse compressive stress tests, the width of the pressure block used was 1.5 or 3 mm. Thus, the voltage sensing leads was connected to the test wire outside its stressed region. The difference between I_c based on the actual tap separation and I_c based on the effective separation (block width) was less than 3 %. The compressive stress was estimated by dividing the applied load by the projected compressive area (wire diameter x block width) excepting the case otherwise described. More than two samples were used for each measurement conditions.

Table 1(a) Specification of wires (Nb matrix)

	Nb_mNb_3Sn	Bz_mNb_3Sn
Wire diameter (mm)	0.75	0.8
Matrix	Nb	13wt%Sn-Cu
Number of filaments	15(7at%Sn-Cu)	5587(Nb)
Filament dia.(mm)	~70	3.4
Bronze/Nb ratio	0.16	4.1
Cu/non Cu ratio	0.18	0.78
Barrier		Ta
Heat treatment	700℃ x 72h	750℃ x 192h

Table 1(b) Specification of wires.(CuNb reinforcing stabilized)

	$(Nb,Ti)_3Sn$	
Sheath	CuNb	Cu
Wire diameter (mm)	0.8	
Superconductor area		
Matrix	Cu-13wt.% Sn	
Filament diameter (μm)	3.4 (Nb-1.2wt.% Ti)	
Number of filament	5587 (151x37)	
Bronze ratio (bronze/Nb)	4.09	
Barrier	Ta	
Cu (+CuNb) to superconductor ratio		
Pure copper	0.14	0.78
CuNb composite	0.63 (20wt.% Nb)	-
Heat treatment	670℃ x 192 h	

3. Results and Discussion

3.1 Nb matrix Nb_3Sn wire

3.1.1 *Axial Tensile Strain Effect of Critical Current*

The stress-strain curves of Nb_m-and Bz_m-Nb_3Sn wires are shown in Fig.2. The 0.2% proof stress of Nb_mNb_3Sn wire is 550 MPa and about 3 times higher than that of Bz_mNb_3Sn wire (160 MPa) and also 2 times higher than that of CuNb/$(Nb,Ti)_3Sn$ (250Mpa) to be described in 3.2.2. The flow stress is also high. This is mainly due to large volume fraction of Nb with high proof stress (1000 MPa at 4.2K).[16]

The strain dependence of I_c normalized to its peak value I_{cm} in a Nb_mNb_3Sn wire measured at the magnetic fields of 6, 10 and 14T are shown in Fig.3, respectively. The result obtained in the Bz_mNb_3Sn wire is also shown in the figure for comparison. The strain sensitivity in

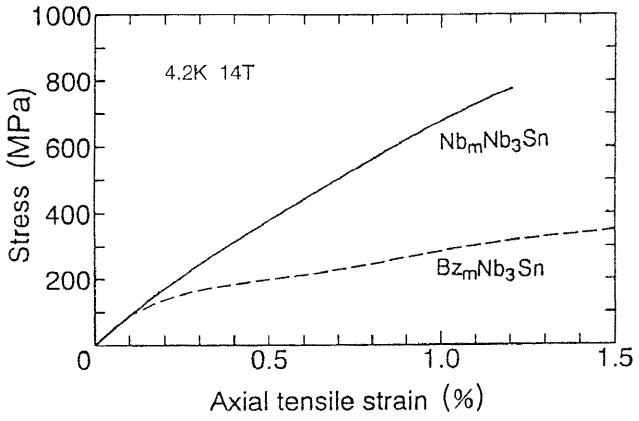

Figure 2 Stress vs. strain curves

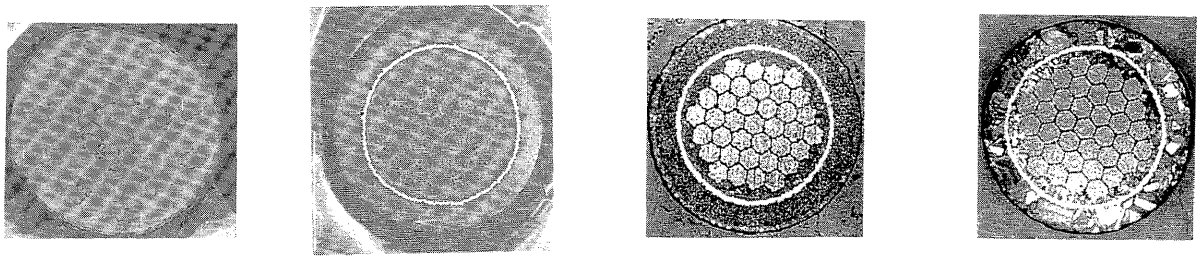

(a) Nb_mNb_3Sn (b) Bz_mNb_3Sn (c) CuNb/$(Nb,Ti)_3Sn$ (d) Cu/$(Nb,Ti)_3Sn$

Figure 1 Cross-sectional view of wires

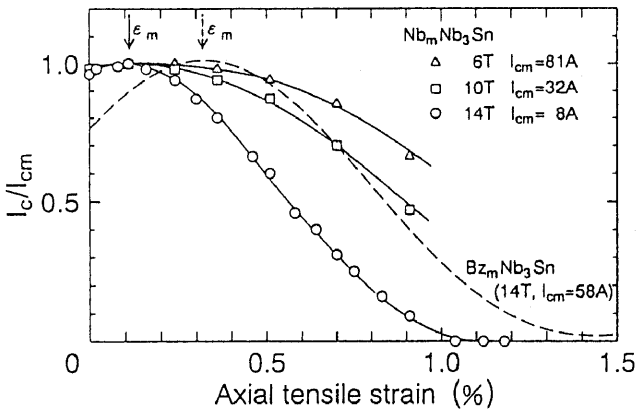

Figure 3 Strain dependence I_c normalized to I_{cm}

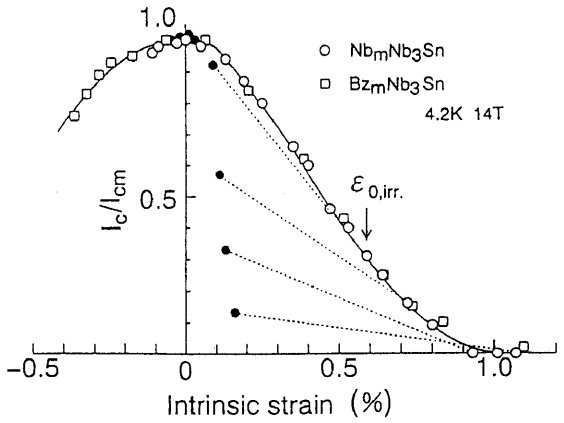

Figure 4 Strain sensitivity of I_c

Nb_mNb_3Sn wire increases with the increase of magnetic field. The strain for the peak of I_c , ε_m , is 0.11% in the Nb_mNb_3Sn wire. It is known that ε_m corresponds to the residual strain in the Nb_3Sn filaments. Because the volume fraction of Nb with low coefficient of thermal contraction is large in the Nb_mNb_3Sn wire, ε_m is smaller than that of Bz_mNb_3Sn wire (0.33 %). Figure4 shows the strain dependence of I_c for both Nb_m- and Bz_m-Nb_3Sn wires, where the intrinsic strain is a net strain in the Nb_3Sn filaments which is obtained by subtraction of ε_m from the applied strain. No appreciable difference between two curves can be seen. This appears to indicate that the Nb_3Sn layers formed in Nb_3Sn wires are almost the same as those in Bz_mNb_3Sn wires, including the changes in the strain state within applied strain.

The reversible strain limit ε_{irr} beyond which the I_c on unloading starts to deviate from the I_c vs strain curve on loading means that some permanent defect are introduced in the Nb_3Sn layer. The ε_{irr} for Nb_mNb_3Sn wire is 0.83% and is almost the same as that in conventional Bz_mNb_3Sn wires (typically 0.6-0.8%).

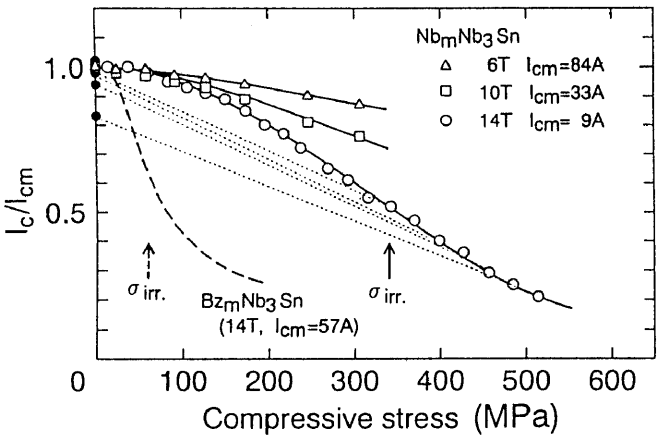

Figure 5 Transverse stress dependence of I_c normalized to I_{cm}

3.1.2 *Transverse Compressive Stress Effect of Critical Current*

The transverse compressive stress dependencies of I_c normalized to the I_{cm} at the magnetic fields of 6, 10 and 14T in Nb_mNb_3Sn wire as well as that in Bz_mNb_3Sn wire at 14T are shown in Fig.5, respectively. I_c degrades monotonically with increase in the stress. The stress dependence is increased with the increase in magnetic field, as in the case of the axial tensile strain effect. The stress which results in the degradation of I_c/I_{cm}=0.9 at 14T is 130 MPa for Nb_mNb_3Sn wire and is 2.2 times higher than that for Bz_mNb_3Sn wire.

It has been already reported that the I_c degradation due to the transverse compressive stress occurs in two stages as in the case in the axial strain effect.[16] One is the stage I where all the constituents behave elastically and I_c recovers reversibly when the applied stress is removed. In the stage II, I_c does not recover to the initial value after unloading. The I_c degradation in the stage II may be attributed to the cracking in the Nb_3Sn filaments and the local permanent deflection of filaments due to plastic deformation of the matrix. For the results obtained on Nb_mNb_3Sn wires, the solid circles in Fig.5 shows the data of I_c on unloading. The boundary stress between the stage I and II, σ_{irr}, is 330 MPa in Nb_mNb_3Sn wire and is higher about 6 times as compared to 60 MPa in the Bz_mNb_3Sn wire. The matrix Nb with higher proof stress appears to sustain higher stress without plastically deforming than the matrix Cu in Bz_mNb_3Sn and also in CuNb/$(Nb,Ti)_3Sn$ wire (σ_{irr}=230MPa) in 3.2.2. Thus, Nb matrix increases the tolerant stress of σ_{irr}. Furthermore, it was confirmed by the experiment that the σ_{irr}, about 320 MPa at 6, 10, 14T, respectively, did not depend on the magnetic field. It indicates that the irreversibility caused by transverse compressive stress mainly is resulted from the mechanical damage to the filaments as in the case of ε_{irr} for the axial

tensile strain effects.

3.1.3 *Comparison Between Axial Tensile Strain Effect and Transvers Compressive Stress Effect*

As described above, the magnitude of the transverse compressive stress effect on I_c strongly depends on the mechanical properties of the matrix material of the composite wires. Thus, the large difference in the magnitude of I_c degradation between Nb_m- and Bz_m-Nb_3Sn wires is mainly resulted from large difference in σ_{irr}. Furthermore it has been confirmed that I_c vs. transverse compressive stress characteristics can be divided into two categories, the reversible stress region (Stage I) and the irreversible stress region (Stage II) and presumably the mechanism of I_c-degradation may not be the same in each region, as in the case of the axial strain effects. Consequently, in making a comparison of the intrinsic magnitude of I_c-degradation between transverse compressive stress and the axial tensile stain, first, it should be made for I_c-degradation in the same category. Secondly, the stress distribution in the wire cross section should be taken into account. The stress analysis reveals that mean stress is 1.8 times higher and the highest stress is about 5 times as compared with the nominal one for Nb-tube processed Nb_3Al wires.[17] The critical current density changes locally depending on the stress distribution.

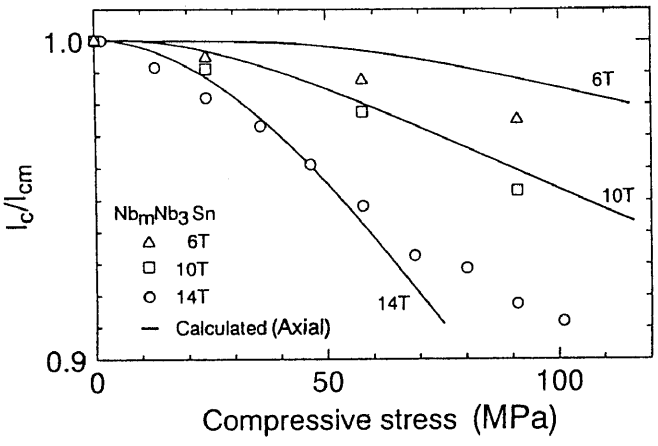

Figure 6 Comparison of I_c degradation in Nb_mNb_3Sn wire for transverse and axial compressive stress

Figure 6 shows the comparison of the axial and transverse stress dependencies of I_c in the reversible stress region in the wire. This comparison of stress dependencies of I_c in the same category of I_c was realized in the Nb_mNb_3Sn wires which show much larger σ_{irr} than conventional Bz_mNb_3Sn wires. The axial stress is derived from the axial strain in Fig.3 by multiplying Young s modulus of 80 GPa[18], and then overall I_c is calculated by summation of the local critical current corresponding to the stress distribution in the cross section of the wire. Here, it is assumed that the Nb matrix behaves elastically and the stress distribution is approximately the same as that derived from a solution for in plane compression of elastic circular plate which has been used in the Nb_3Al wire already reported[17]. The coincidence between the transverse stress effect of I_c measured and that derived from calculation based on the axial tensile strain effect of I_c indicates that stress dependence of I_c is essentially identical for both axial and transverse direction in the Nb_mNb_3Sn wire. Similar results have been reported in the case of Nb_3Sn tape[19] and Nb_3Al wire[17].

The "σ_{irr}" for axial tensile stress effects in Nb_mNb_3Sn is derived to be 576 MPa from ε_{irr} multiplying Young's modulus 80 GPa. This value is close to 594MPa the "effective" irreversible transverse compressive stress, obtained by multiplying 1.8, the ratio mentioned above, to 320MPa. This coincidence, however, is fortuitous because 1) σ_{irr} in the transverse compression is to be controlled mainly by the maximum stress in the cross section of wire and the ratio of the maximum stress to the nominal σ_{irr} should be 5, if the configuration of the filaments for Nb_mNb_3Sn and Nb-tube processed Nb_3Al wires is the same, 2) the magnitude of the tensile stress component which results in the filament fracture in the axial tensile stress effect is different from that in the transverse compressive stress effect.

3.2 CuNb Reinforcing stabilized Nb_3Sn wire

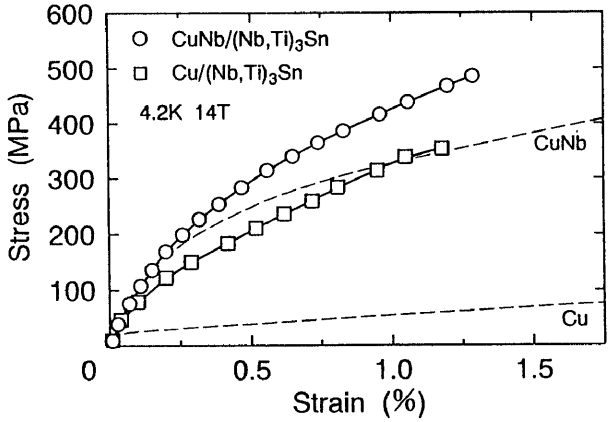

Figure 7 Stress-strain curves of CuNb, Cu and supercon ducting wires

3.2.1 *Axial Tensile Strain Effect on Critical Current*

The stress-strain curves of the superconducting wires at 14T, 4.2K are shown in Fig.7. Remarkable increases in the 0.2% proof stress from 170 to 250 MPa and the flow stress are induced by replacing the Cu stabilizer with the CuNb reinforcing stabilizer. In Fig.7, the stress-strain curves of CuNb (20wt% Nb) and Cu wires, constituting

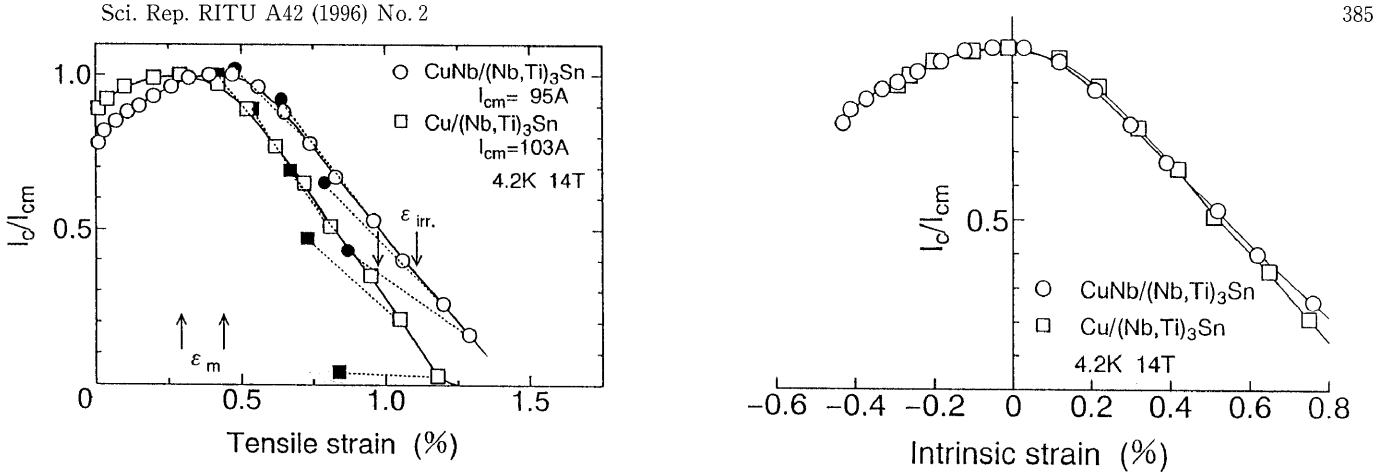

(a) as a function of applied strain ε (b) as a function of intrinsic strain $\varepsilon_0=\varepsilon-\varepsilon_m$

Figure 8 Strain dependence of I_c normalized by its maximum I_{cm} in the superconducting wires.

materials for fabrication of the superconducting wires, are also shown. Significant difference in the curves which results in the marked reinforcing effect of the composites can be seen.

The strain dependence of I_c in the CuNb/(Nb,Ti)$_3$Sn wire is compared with that in the Cu/(Nb,Ti)$_3$Sn (Fig.8(a)). The ε_m is shifted from 0.29 to 0.43% when the Cu is replaced by the CuNb. This is attributed to an increase in the proof stress of the stabilizer. The ε_{irr} is about 0.95 % in Cu/(Nb,Ti)$_3$Sn wire. This is also shifted almost the same amount of strain as that in the ε_m by the reinforcement. The strain sensitivity of I_c for both wires are eventually identical, as shown in Fig.8(b).

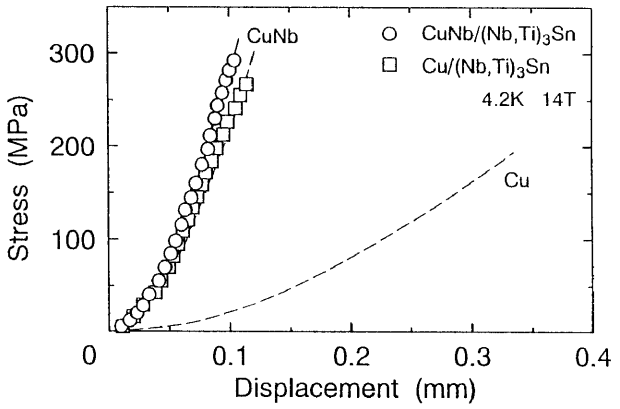

Figure 9 Transverse compressive stress-displacement curves of CuNb, Cu and superconducting wires

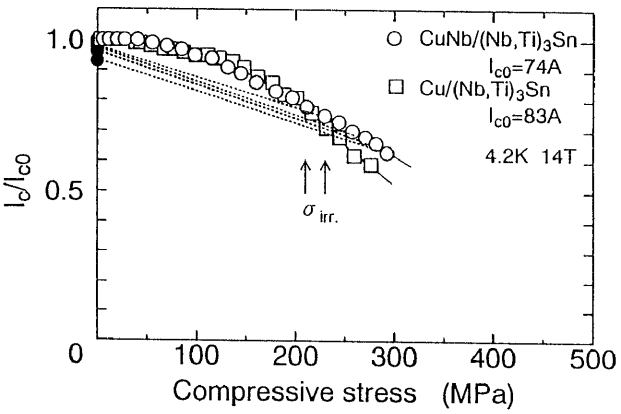

Figure 10 Transverse compressive stress dependence of I_c normal-ized by its maximum I_{cm} in the superconducting wires.

3.2.2 *Transverse Compressive Stress Effect on Critical Current*

Figure 9 shows the transverse compressive stress vs. displacement relation in the CuNb/(Nb,Ti)$_3$Sn and Cu/(Nb,Ti)$_3$Sn. Due to the difference in the compressive behavior between CuNb and Cu, as can be seen in Fig.10, the pair of superconducting composites shows substantially different behavior resulted from both the deformation in the outer shell and that in the superconducting area, respectively.

The transverse compressive stress dependencies of I_c normalized by that at its zero applied stress, I_{c0}, at the magnetic field of 14 T in the superconducting wires are shown in Fig.10. I_c decreases monotonically with an increase in the stress.[20, 21]

In Fig.10, it can be seen that the stress sensitivity of I_c in stage I decreases by reinforcing Cu with Nb submicron-filaments. The outer shell of CuNb with high rigidity supports the transverse compressive load and therefore the stress transferred to the interior superconducting area would be small. The solid circles in Fig.10 show the data of I_c on unloading in CuNb/(Nb,Ti)$_3$Sn wires. The boundary stress between stages I and II, σ_{irr}, is 230 MPa in the CuNb/(Nb,Ti)$_3$Sn wire and is higher about 1.1 times as compared with 210 MPa in the Cu/(Nb,Ti)$_3$Sn. Here, we can see that the reinforcing stabilizer improves the σ_{irr} and the stress sensitivity of I_c in the region of stage II.

3.2.3 *Damages Induced by Transverse Compressive Stress*

In order to investigate the microscopic aspects of the damages induced by the transverse compressive stress,

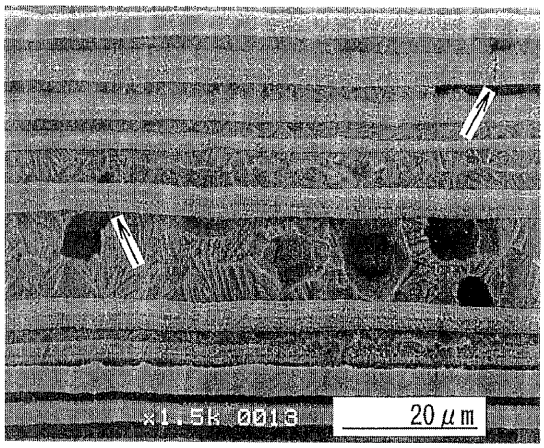

Figure 11 Longitudinal section of CuNb/$(Nb,Ti)_3Sn$ wire compressed transversely (260MPa)

both the cross section and the longitudinal section of the wires were polished, etched and then examined using an optical microscope and a scanning electron microscope. In the cross section of the CuNb/$(Nb,Ti)_3Sn$ wire, we can see a depression on the top of the wire where the pressure block pushed until I_c/I_{c0} degrades to 0.7 (260 MPa), beyond the σ_{irr}.

Fig.11 shows cracks distributed randomly along the filaments in the longitudinal section and in their magnified view. They are different from evenly spaced cracks[22]. Density of the cracks at the edge part of the pressure block is almost the same as that in the flat part. Although strain concentration at the edge of the pressure block may induce some discrepancy with the transverse compressive stress effect data obtained by excluding the edge effect[21], the difference, however, does not appear to be significant. This is consistent with that I_c degradation in the concentrated condition is eventually not so different from that in uniform stress[23], although some effect of pressure block width on I_c was reported[24]. I_c degradation beyond the σ_{irr} is thus resulted from the residual strain and cracking in the Nb_3Sn filaments caused by plastic deformation in the matrix and outer shell.

3.2.4 *Comparison Between Axial Tensile Strain Effect and Transverse Compressive Stress Effect*

It has been shown that the CuNb reinforcing stabilizer drastically changes the mechanical properties and I_c vs. strain characteristics when the wires are loaded in the axial direction. According to the I_c vs. transverse compressive stress behaviors mentioned in the preceding section, however, the difference between them is not so much, although a significant difference in the mechanical behavior can be seen. This indicates that the difference in the deformation within the superconducting area is comparatively small. Thus the role of reinforcing CuNb in the transverse compression is significantly different from that in the axial tension. In the transverse compression test, it acts as a shell structural component. Further, the mechanical behavior of CuNb micro-composite is anisotropic and reinforcement by filaments appears to be less effective to the transverse compressive stress.

Within a limited range of loading, where the matrix within the superconducting area behaves apparently elastically, the comparison is made between the axial stress dependence and the transverse compression stress dependence of I_c in the different way as in the case of the Nb matrix Nb_3Sn superconducting wires (3.1.3). Here, we suppose only the geometric average strain $< \varepsilon >$, one representation of distortional strain given as eq. (2),[21] controls the degradation of I_c under multiaxial strain condition.

$$< \varepsilon > = 2^{-1/2}(1+\nu)^{-1}[(\varepsilon_x-\varepsilon_y)^2+(\varepsilon_y-\varepsilon_z)^2+(\varepsilon_z-\varepsilon_x)^2]^{1/2} = 2^{-1/2}E^{-1}[(\sigma_x-\sigma_y)^2+(\sigma_y-\sigma_z)^2+(\sigma_z-\sigma_x)^2]^{1/2} \quad (2)$$

where ν is poisson's ratio, E is Young s modulus ε_x, ε_y and ε_z are the strain components along the major axes in the elastic material and $< \varepsilon >$ is also expressed in terms of the stress components σ_x, σ_y and σ_z in a elastic material.

Taking x axis along the longitudinal direction of wire and y axis transverse compressive direction, and supposing thermal residual stresses in the radial and circumferential directions within the wire can be ignored, $< \varepsilon >$ in the wire is simply a function of σ_x and σ_y. We use average σ_y derived by multiplying 1.8 to the nominal applied transverse compressive stress[17] and 109 GPa for E in the $(Nb,Ti)_3Sn$[25]. Figure12 shows an I_c vs. $< \varepsilon >$ relation for both the axial tensile test and the transverse compressive test. The tensile test data for each wires give two lines corresponding with positive and negative intrinsic strain region, respectively. The I_c data for the transverse compressive tests start from each negative ends of the lines for tensile test, i.e. in axially compressed stress states. Al-

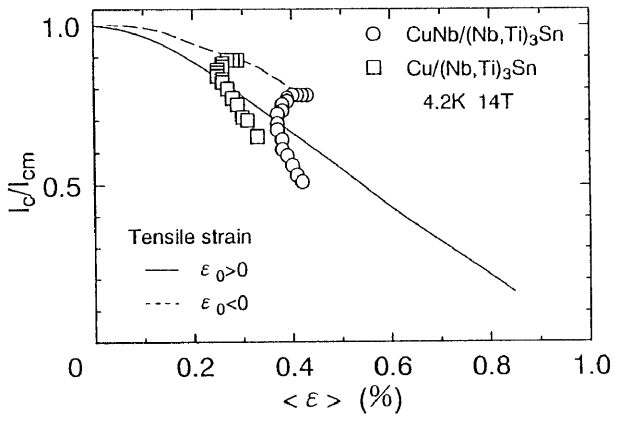

Figure 12 I_c normalized by its maximum I_{cm} as a function of geometric average strain <ε> in CuNb /$(Nb,Ti)_3Sn$ and Cu/$(Nb,Ti)_3Sn$ wires.

though a discrepancy between both is relatively small in the Cu/(Nb,Ti)$_3$Sn wire, a large difference is seen in the CuNb/(Nb,Ti)$_3$Sn wire, where the initial compressive stress is high. This appears to indicate that the degradation of I_c in stage I stress region by axial tensile stress and one by transverse compressive stress can not be simply described by the same mechanical parameter using rough estimation mentioned above.

4. Conclusions

Axial tensile and transverse compressive tests of high strength bronze processed Nb_3Sn wires, namely Nb matrix wires [Nb_mNb_3Sn] and wires reinforcing stabilized by a CuNb composite [CuNb/(Nb,Ti)$_3$Sn] were conducted in magnetic fields up to 14T at 4.2K. Changes in the critical current I_c in the wires were evaluated. Following results were obtained.

Nb matrix wires

1. The 0.2% proof stress of Nb_mNb_3Sn wire is 550 MPa and is 3.4 times larger as compared with that (160 MPa) in the conventional wire.
2. The strain for the peak value of I_c in the axial strain dependence of I_c in Nb_mNb_3Sn wire 0.11% is smaller than that (0.33%) in the conventional wire. No difference in the strain sensitivity between them can be seen..
3. The transverse stress dependence of I_c in Nb_mNb_3Sn wire is low as compared with that in the conventional wire. The irreversible transverse compressive stress for I_c, σ_{irr}, does not depend on the magnetic field. The σ_{irr} in the Nb_mNb_3Sn wire is 330 MPa and is 6 times higher than that (60 MPa) in the conventional wire.
4. The transverse compressive stress dependence and the axial tensile stress dependence of I_c in the reversible stress region in the Nb_mNb_3Sn wires are almost the same in magnitude, if the transverse stress distribution within the cross section of the wire is taken into account.

CuNb reinforced wires

5. The 0.2% proof stress of the CuNb/(Nb,Ti)$_3$Sn wire is 250 MPa and is 1.5 times larger as compared with that 170 MPa in the Cu/(Nb,Ti)$_3$Sn wire.
6. The strain for the peak value of I_c in the axial strain dependence of the CuNb/(Nb,Ti)$_3$Sn wire (0.43%) is larger than that of the Cu/(Nb,Ti)$_3$Sn wire (0.29%). No difference can be seen in the strain sensitivity of I_c between them.
7. The transverse stress sensitivity of I_c in the CuNb/(Nb,Ti)$_3$Sn wire is slightly lower than that in the Cu/(Nb,Ti)$_3$Sn wire. The σ_{irr} in the CuNb/(Nb,Ti)$_3$Sn wire is 230 MPa and is about 1.1 times higher than 210 MPa in the Cu/(Nb,Ti)$_3$Sn. These are due mainly to the configuration of the CuNb in the wire associated with the loading direction and partly to the anisotropy in the mechanical properties of CuNb.

In Summary, CuNb/(Nb,Ti)$_3$Sn wires with a high critical current density and strength is now practically applicable. Although the critical current density and stability are not high enough at this moment, further strength is attained in the Nb_mNb_3Sn matrix wires..

Acknowledgment

The authors wish to express their thanks to H.S. Shin, Y. Shoji, H. Seto, N. Ebisawa in Iwate University for their assistance in the experiment. This work was carried out at the High Field Laboratory for Superconducting Materials, Institute for Material Research, Tohoku University. They appreciate many assistance by the staffs.

1) J.W. Ekin, R. Flükiger ,and W. Specking, J. Appl. Phys., **54**(1983), p.2869
2) R. Flükiger, E. Drost ,and W. Specking, Adv. Cryog. Eng., **30**(1984), p.875
3) K. Noto, N. Konishi, K. Watanabe, A. Nagata, and T. Anayama, in "Proc. Int. Symp.Flux Pin. Electromagn. Prop. Superconds.", Eds. T. Matsushita, K. Yamafuji, and F. Irie, Matsukuma Press, Fukuoka (1985), p.272.
4) R. Flükiger, and A. Nyilas, IEEE Trans. Magn., MAG-**21** (1985), p.285.
5) S. Nakayama, S. Murase, K. Shimamura, N. Aoki, and N. Shiga, Adv. Cryog. Eng., **38**(1992), p.279.
6) M. Matsukawa, K. Noto, C. Takahashi, Y. Saito, N. Matsuura, K. Katagiri, M. Ikebe, T. Fukutsuka, and K. Watanabe, IEEE Trans. Magn., **28**(1992), p.880.
7) E. Gregory, L.R. Motowidlo, G.M. Ozeryansky, and L.T. Summers, IEEE Trans. Magn., MAG-**27**(1991) p.2033.
8) C.C. Tsuei, J. Appl. Phys., **45**(1974), p.1385.
9) J. Bevk, J.P. Harbison, and J.L. Bell, J. Appl. Phys., **49** (1978), p.6031.
10) C.V. Renaud, E. Gregory, and J. Wong, Adv. Cryog. Eng., **32**(1986), p.443.
11) K. Watanabe, S. Awaji, K. Katagiri, K. Noto, K. Goto, M. Sugimoto, T. Saito, and O. Kono, IEEE Trans. Magn., **30**(1993), p.1871.
12) K. Katagiri, K. Watanabe, K. Noto, K. Goto, T. Saito, O. Kono, A. Iwamoto, M. Nunogaki, and T. Okada, Cryogenics, **34**(1994), p.1039.
13) K. Katagiri, T. Kuroda, H. Wada, H.S. Shin, K. Watanabe, K. Noto, Y. Shoji , and H. Seto, IEEE Trans. Applied Superconductivity, **5**(1995) in press .
14) K. Katagiri, M. Fukumoto, K. Saito, M. Ohgami, T.

Okada, A. Nagata, K. Noto, and K. Watanabe, Adv. Cryog. Eng., **36**(1990), p.69.

15) K. Kamata, K. Katagiri, T. Okada, T. Takeuchi, K. Inoue, K. Watanabe, Y. Muto, T. Ogata, and T. Tsuji, in "Proc. 11th Int. Conf. Magnet Tech." Eds. T. Sekiguchi, and S. Shimamoto, Elsevier Appl. Sci., London (1989), p.1231.

16) T. Kuroda and H. Wada, Cryogenic Eng., **28**(1993), p.439 (in Japanese).

17) T. Kuroda, H. Wada, S.L. Bray, and J.W. Ekin, Fusion Eng. and Design, **20**(1993), p.271.

18) K. Watanabe, K. Katagiri, N. Noto, S. Awaji et al, Preprint Spring Mtg. Cryog. Eng. Jpn, (1994), p.137 (in Japanese).

19) B.ten Haken, A. Godake and H.H.J. ten Kate, Adv.Cryog. Eng., **40**(1994), p.875.

20) W. Specking, W. Goldacker, and R. Flukiger, Adv. Cryog. Eng., **34**(1988), p.369.

21) J.W. Ekin, J. Appl. Phys. , 62(1987), p.4829

22) H. Boschman, A.P. Verweij, S. Wessel, H.H.J. ten Kate, and L.J.M. van de Klundert, IEEE Trans., MAG-**27** (1991), p.1831.

23) S.L. Bray and J.W. Ekin, Adv. Cryog. Eng., **38**(1992), p.643.

24) H. Boschman and L.J.M. van de Klundert, Adv. Cryog. Eng., **36**(1990), p.93.

25) F.J. Bussiere, B. Faucher, C.L. Snead Jr., and M. Suenaga, Adv. Cryog. Eng., **28**(1982), p.453